

Properties of Coexisting Phases for the Ethanol–Ethane Binary System by Computer Simulation

I. Yu. Gotlib and E. M. Piotrovskaya*

Department of Chemistry, St. Petersburg State University, Universitetsky pr., 2, Petrodvorets, St. Petersburg 198904, Russia

Received: January 22, 1999; In Final Form: June 3, 1999

Thermodynamic properties (configurational energies, compositions, densities) and structural characteristics of coexisting liquid and vapor phases in the ethanol–ethane binary system at the temperature 348.15 K in the pressure range 1.70–7.83 MPa are calculated by the Gibbs ensemble Monte Carlo method. Obtained values are in satisfactory agreement both with the experimental data and the results of the application of the hole quasichemical group-contribution model (at pressures far enough from the critical point). The calculated phase diagram at 348.15 K agrees satisfactorily with the experimental one; the value of the critical pressure obtained from simulations is about 13% lower than that from the experiment.

Introduction

This work, in which the properties of an ethanol–ethane binary mixture are calculated by the Gibbs ensemble Monte Carlo method, is the continuation of the previous works^{1–3} on the simulation of systems containing lower hydrocarbons and alcohols. In the present work, the properties of coexisting liquid and vapor phases in the $\text{C}_2\text{H}_5\text{OH}-\text{C}_2\text{H}_6$ binary system are studied by NpT Gibbs ensemble Monte Carlo simulation. As well as the $\text{CH}_3\text{OH}-\text{C}_2\text{H}_6$ system studied in,³ the $\text{C}_2\text{H}_5\text{OH}-\text{C}_2\text{H}_6$ system is a relatively simple system containing a nonpolar component (hydrocarbon) and a polar one capable of forming hydrogen bonds (alcohol). Additionally, the molecule of alcohol contains a polar part (hydroxyl group) and a nonpolar hydrocarbon tail. The properties of alcohol–hydrocarbon systems, including phase behavior, strongly depend on the tail length. Thus, the phase diagram of a methanol–ethane system (where the hydrocarbon tail of the molecule of alcohol is the shortest) is rather complicated and includes liquid–liquid phase separation, while an ethanol–ethane system shows total liquid–liquid miscibility below the critical temperature of C_2H_6 (305.5 K).^{4,5}

As far as we know, there are no published works on computer simulation of the $\text{C}_2\text{H}_5\text{OH}-\text{C}_2\text{H}_6$ binary system. Monte Carlo (MC) and molecular dynamics (MD) simulations of ethane were performed in several studies, in particular, ref 6; the C_2H_6 model potential parameters used by us are taken from that work. Ethanol, along with other lower alcohols, was studied using NpT MC method by Jorgensen.⁷ Recently, van Leeuwen⁸ held Gibbs ensemble MC simulations of several alcohols (ethanol, 1-propanol, 2-propanol, 1-hexanol, 3-hexanol); this technique allowed to calculate simultaneously the properties of coexisting liquid and vapor phases and to estimate critical temperatures and pressures for pure alcohols. The author of ref 8 studied the applicability of the site–site Lennard–Jones model potential, based on a “fully transferable” (uniform) set of parameters for CH_n ($0 \leq n \leq 3$) and hydroxyl groups in homologous alkanes and alkanols, for the prediction of the densities of coexisting phases and vaporization enthalpies for pure alkanols (ethanol, 1-propanol, 2-propanol, 1-hexanol, 3-hexanol). In that work, van

Leeuwen obtained quite satisfactory results for pure ethanol and propanols; however, for hexanol isomers some additional tuning of parameters was needed. The set of potential parameters, used by van Leeuwen in ref 8, was developed on the basis of Jorgensen’s studies;⁷ in the present work, the model potential for $\text{C}_2\text{H}_5\text{OH}$ is principally the same as in refs 7 and 8. Additionally, one can mention two recent works where molecular simulation results for ethanol have been reported: Gao et al.⁹ used the NpT MC method and a “polarizable” intermolecular model potential for several lower liquid alcohols, thus having reproduced, in principle, Jorgensen’s simulations with another potential model in which polarization effects were taken into account; Padró et al.¹⁰ performed MD calculations of thermodynamic properties and structural characteristics of $\text{C}_2\text{H}_5\text{OH}$ at four temperatures from 173 K to 348 K with the same model potential as Jorgensen and van Leeuwen.

The aim of this work was to extend this approach to the simulation of the binary system $\text{C}_2\text{H}_5\text{OH}-\text{C}_2\text{H}_6$, to test the applicability of such a simple model potential for the prediction of properties of coexisting phases in the alkanol–alkane system, within the framework of the Gibbs ensemble MC method, thus extending to a binary amphiphilic system the method which proved itself to be quite successful, in particular, for pure lower alcohols. This is the most direct method of calculating, in a computer experiment, properties of both coexisting phases of a system, and testing its advantages and limitations is of significant interest.

Models, Simulation Conditions and Details

We chose a simulation temperature, 348.15 K, that is higher than the critical point of ethane; the pressure–composition diagram of the $\text{C}_2\text{H}_5\text{OH}-\text{C}_2\text{H}_6$ system at 348.15 K has an ordinary “droplike” shape.⁵ The experimental critical pressure, where two coexisting phases become identical, is 9.66 MPa at this temperature; the molar content of ethane in the critical phase is $x_{\text{C}_2\text{H}_6} = 0.7520$.⁵

Simulation pressure p changes in the range from 1.70 MPa to 7.83 MPa; chosen values of p are those for which experimental data are given in ref 5.

* E-mail: elena@nonel.chem.lgu.spb.su.

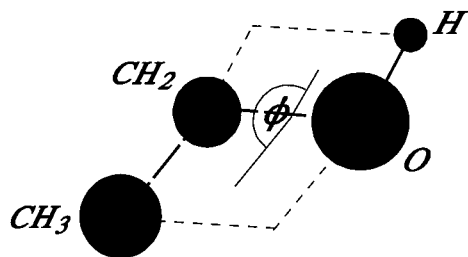


Figure 1. Ethanol molecule model.

TABLE 1: Model Values of Lennard–Jones Interaction Parameters and Coulomb Point Charges, Bond Lengths L and Angles φ^a

group	$(\epsilon/k)/\text{K}$	σ/nm	$q/ e ^b$
CH ₃ (ethane)	139.81	0.3512	
CH ₃ (ethanol)	88.06	0.3905	
CH ₂ (ethanol)	59.38	0.3905	0.265
O (ethanol)	85.55	0.307	−0.700
H (ethanol)			0.435

bond	L/nm
CH ₃ –CH ₃ (ethane)	0.2353
CH ₃ –CH ₂ (ethanol)	0.153
CH ₂ –O (ethanol)	0.143
O–H (ethanol)	0.0945

bond	φ/deg
CH ₃ –CH ₂ –O (ethanol)	108
CH ₂ –O–H (ethanol)	108.5

^a The parameters of ethane are from refs 6, 14, the parameters of methanol are from ref 8. ^b e is the charge of an electron.

The description of intermolecular interactions by means of relatively simple atom–atom model potentials proved itself to be quite appropriate for calculating properties of different molecular systems, including those containing hydrocarbons and/or alcohols. Therefore, we use this approach. C₂H₆ is described as a diatomic Lennard–Jones molecule with the parameters of model potential taken from ref 6; in ref 6, an excellent agreement between the results of molecular dynamics simulation and the experimental pressure–temperature diagram was obtained for temperatures both below and above the critical point of ethane (although it should be noted that the value of the critical temperature calculated using the NpT molecular dynamics plus test particle method¹¹ with these parameters for ethane is too high (326.6 K), and recently somewhat modified values of the parameters were used in the simulations of ref 12). The C₂H₅–OH molecule is considered to include three Lennard–Jones centers (CH₃ group, CH₂ group, and oxygen atom) and three Coulomb point charges (CH₂ group and atoms O and H); additionally, torsional energy was taken into account for ethanol

$$U^{\text{tors}}(\phi) = V_0 + \frac{V_1}{2}(1 + \cos\phi) + \frac{V_2}{2}(1 - \cos 2\phi) + \frac{V_3}{2}(1 + \cos 3\phi) \quad (1)$$

where ϕ is the dihedral angle between the CH₃–CH₂–O and CH₂–O–H planes (Figure 1). This equation, based on the Fourier expansion, was used in both ref 7 and 8. The values of Coulomb charges and Lennard–Jones interaction parameters for interaction centers of identical kind, and also bond lengths and angles, are given in Table 1. Torsional potential parameters for the ethanol molecule are (in kJ/mol) $V_0 = 0$; $V_1 = 3.489$; $V_2 = (-0.485)$; $V_3 = 3.125$.

Lorentz–Berthelot rules are used for interactions between Lennard–Jones “atoms” (centers) of different kind

$$\epsilon_{\alpha\beta} = \sqrt{\epsilon_{\alpha\alpha}\epsilon_{\beta\beta}} \quad (2)$$

$$\sigma_{\alpha\beta} = \frac{\sigma_{\alpha\alpha} + \sigma_{\beta\beta}}{2} \quad (3)$$

These rules were the same as those used by van Leeuwen,⁸ while Jorgensen in ref 7 assumed $\sigma_{\alpha\beta} = \sqrt{\sigma_{\alpha\alpha}\sigma_{\beta\beta}}$.

Total energy of the system is the sum of the Lennard–Jones and Coulomb particle interaction energies and torsional energy of ethanol molecules. A spherical cutoff is used for molecular interactions: if the distance between the “base points” of two molecules (CH₂ groups of C₂H₅OH molecules or centers of C₂H₆ molecules) is more than 2.5 times greater than σ for the methylene group of ethanol, the interaction energy is considered to be zero. The applicability of such a cutoff procedure was discussed in ref 3 (see also ref 13). Particularly, our experience with the simulation of the CH₃OH–C₂H₆ system³ showed that including long-range electrostatic interactions into the model potential by means of the Ewald summation procedure gave no real improvement of the calculated values of thermodynamic properties.

The total number of particles in the model system is as follows: at $p = 1.70$ MPa, 896 (800 C₂H₅OH molecules and 96 C₂H₆ molecules); at $p = 7.83$ MPa, 1728 (528 C₂H₅OH molecules and 1200 C₂H₆ molecules); at other pressures, 1120 (800 C₂H₅OH molecules and 320 C₂H₆ molecules at $p = 3.77$ MPa and $p = 5.29$ MPa, 640 C₂H₅OH molecules and 480 C₂H₆ molecules at $p = 6.56$ MPa). This is based on rather obvious considerations: the closer to the critical state, the greater the total number of particles required in order to obtain reliable enough results for a simulated system; fixing higher total content of C₂H₆ molecules in the whole system at higher pressures is reasonable, as in the real ethanol–ethane system where ethane concentration in the liquid phase increases significantly with increasing pressure, while vapor composition changes only slightly, C₂H₆ concentration in the vapor phase remaining close to 100%.

Periodic boundary conditions are used in all three dimensions.

The number of configurations generated in the simulation process varies from 10^7 (at $p = 1.70$ MPa) to 3×10^7 (at $p = 7.83$ MPa). Averaging is made over 2×10^6 to 5×10^6 configurations. The simulation algorithm is the same as in ref 3.

The simulation results are compared not only with the experimental data but also with the results given by the hole quasichemical group-contribution model (HQGCM). The HQGCM calculation technique was developed by Smirnova and Victorov;^{15,16} the values of the HQGCM parameters used here are taken from ref 17.

Results and Discussion

For coexisting phases, we calculate densities, compositions, configurational energies, conformational distributions of ethanol molecules, atom–atom correlation functions, and hydrogen bonding characteristics for C₂H₅OH molecules. Conformational distribution is presented in the form of the function $\nu(\phi) = 2\pi(\Delta n(\phi))/\Delta\phi$, where $\Delta n(\phi)$ is the fraction of molecules with the torsional angle in the range from $\phi - \Delta\phi/2$ to $\phi + \Delta\phi/2$. H-Bonding association is characterized by the average number of hydrogen bonds per molecule n_{av} and the fractions α_n of molecules forming n hydrogen bonds, $0 \leq n \leq 3$. The same

TABLE 2: Thermodynamic Properties of Coexisting Phases in an Ethanol–Ethane Binary System at 348.15 K: Ethane Molar Content $x_{\text{C}_2\text{H}_6}$, Configurational Energy E_{conf} (kJ/mol), and Molar Volume V (cm³/mol)^a

p/MPa	source	$x_{\text{C}_2\text{H}_6}$		E_{conf}		V	
		liquid	vapor	liquid	vapor	liquid	vapor
1.70	MC results	0.086 ± 0.004	0.91 ± 0.04	-30.5 ± 0.2	-0.4 ± 0.2	66.2 ± 0.6	1500 ± 320
	HQGCM	0.0653	0.9372				
	experiment	0.0639				64.5	
3.77	MC results	0.158 ± 0.007	0.92 ± 0.02	-28.4 ± 0.3	-2.0 ± 0.2	66.4 ± 0.9	570 ± 50
	HQGCM	0.1594	0.9643				
	experiment	0.1553				65.7	
5.29	MC results	0.192 ± 0.007	0.95 ± 0.02	-28.1 ± 0.3	-2.3 ± 0.3	66.7 ± 0.4	340 ± 40
	HQGCM	0.2390	0.9684				
	experiment	0.2366				67.0	
6.56	MC results	0.28 ± 0.02	0.93 ± 0.03	-26.1 ± 0.5	-3.0 ± 0.6	68.9 ± 0.6	230 ± 40
7.83	MC results	0.52 ± 0.03	0.93 ± 0.02	-19.3 ± 0.7	-6.4 ± 0.8	74.8 ± 1.5	120 ± 15
	HQGCM	0.3963	0.9540				
	experiment	0.4094				70.7	
8.5	HQGCM	0.4276	0.9276				
9.15	experiment		0.8870				
9.4	HQGCM	0.4580	0.8998				
	experiment	0.5867					
9.44	experiment		0.8482				
9.62	HQGCM	0.4648	0.8940				
	experiment	0.6746					

^a MC results and hole quasichemical group-contribution model (HQGCM) results obtained in the present work, together with the experimental data,⁵ are presented. Experimental molar content of ethane in vapor in the pressure range 2.00–8.00 MPa is 0.94–0.97; the experimental critical point is: $p = 9.66$ MPa, $x_{\text{C}_2\text{H}_6} = 0.7520$, $V = 82.8$ cm³/mol. For pure ethanol at 350 K, Gibbs ensemble MC simulation⁸ gives $V = (65.0 \pm 0.7)$ cm³/mol, $E_{\text{conf}} = -(34.0 \pm 0.5)$ kJ/mol for the liquid, $V = (22 \pm 6) \times 10^3$ cm³/mol for the vapor.

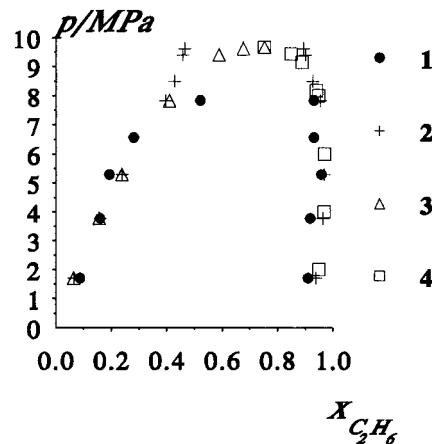
TABLE 3: Hydrogen Bonding Characteristics for C₂H₅OH Molecules in the Liquid Phase at $x_{\text{C}_2\text{H}_6} = 0.086$ ($p = 1.70$ MPa) and at $x_{\text{C}_2\text{H}_6} = 0.52$ ($p = 7.83$ MPa) Calculated by the Gibbs Ensemble MC Method; for Comparison, the Analogous Data from Reference 3, for Pure Methanol and for Methanol–Ethane Liquid Phase at $T = 298.15$ K ($p = 3.7$ MPa, $x_{\text{C}_2\text{H}_6} = 0.24$), Are Also Given

$x_{\text{C}_2\text{H}_6}$	n_{av}	α_0	α_1	α_2	α_3
Ethanol–Ethane System					
0.086	1.66 ± 0.03	6.0 ± 0.5	27.5 ± 1.1	60.8 ± 1.0	5.6 ± 0.8
0.52	1.61 ± 0.04	8.2 ± 1.3	27 ± 2	61 ± 2	4.3 ± 0.9
Pure Methanol and Methanol–Ethane System					
0	1.805 ± 0.035	2.3 ± 1.0	22.1 ± 2.6	68.7 ± 3.0	6.9 ± 1.0
0.24	1.81 ± 0.03	2.1 ± 1.0	18.4 ± 2.5	75.5 ± 2.5	3.7 ± 1.1

energetic criterion of hydrogen bonding as in ref 7 is used: two C₂H₅OH molecules are considered to form a hydrogen bond when their interaction energy is less than -3 kcal/mol.

The simulation results, along with the experimental data, are given in Table 2 (thermodynamic properties) and Table 3 (hydrogen bonding characteristics for liquid at $p = 1.70$ MPa and $p = 7.83$ MPa). The composition–pressure phase diagram at 348.15 K is presented in Figure 2. Different atom–atom correlation functions are shown in Figures 3 and 4. Figure 5 shows the conformational distribution functions $\nu(\phi)$ for ethanol molecules at $p = 1.70$ MPa and $p = 7.83$ MPa.

One can see (Figure 2) that the results obtained for the pressures 1.70 MPa, 3.77 MPa, 5.29 MPa, and 6.56 MPa are in reasonable agreement with the experimental values of the compositions of coexisting phases and liquid density, as well as with the results given by the hole quasichemical group-contribution model. At higher pressures, closer to the experimental critical point, the differences with the experiment become greater. It should be noted that these differences have opposite character for the Gibbs ensemble MC and HQGCM results. Rough extrapolation of the simulation results gives the approximate value of the critical pressure 8.4 MPa, about 13% lower than the experimental one. Meanwhile, as it can be seen from Figure 2, the hole quasichemical group-contribution

**Figure 2.** “Pressure–composition” phase diagram for ethanol–ethane system at 348.15 K: (1) MC simulation results; (2) results calculated using hole quasichemical group-contribution model; (3) the experimental data for the liquid phase;⁵ (4) the experimental data for the vapor phase.⁵

approach does not reveal any sign of the system getting closer to the critical point for pressures up to 9.62 MPa. In fact, HQGCM gives the critical pressure at about 15 MPa. One can notice that the authors of ref 16, having calculated phase behavior for alcohol–hydrocarbon systems with liquid–liquid equilibria, found that HQGCM tended to overestimate the composition differences between two coexisting phases, leading, in particular, to a too high estimated value of the liquid–liquid equilibrium upper critical temperature in a methanol–hexane system. Here HQGCM gives similar deviations from the experiment for the liquid–vapor equilibrium in the C₂H₅OH–C₂H₆ system.

It should be noted that increasing differences with experiment and instability of calculated results when entering critical region are natural for computer simulation, although the Gibbs ensemble MC technique combined with careful control of model system size allowed to estimate critical parameters for simple systems (a Lennard–Jones fluid) with accuracy better than 1%.¹⁸

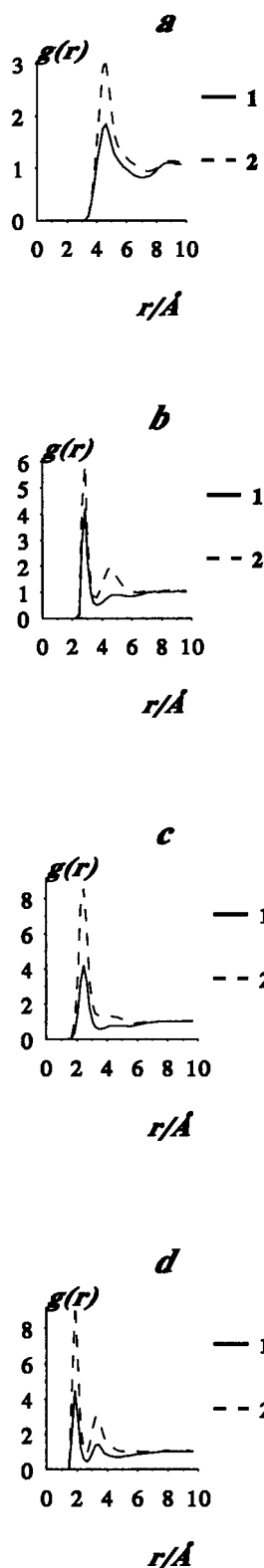


Figure 3. $\text{CH}_2\text{-CH}_2$ (a), O-O (b), H-H (c), O-H (d) correlation functions for ethanol molecules: (1) in the liquid phase at $p = 1.70$ MPa ($x_{\text{C}_2\text{H}_6} = 0.086$); (2) in the liquid phase at $p = 7.83$ MPa ($x_{\text{C}_2\text{H}_6} = 0.52$).

The main problem is that, to obtain thermodynamically correct results for such systems in the near-critical region, the number of particles in two subsystems representing coexisting phases should be only slightly different (in the ideal case, they should be equal);¹⁹ for systems with two or more components, this requirement will refer to the total number of particles in each

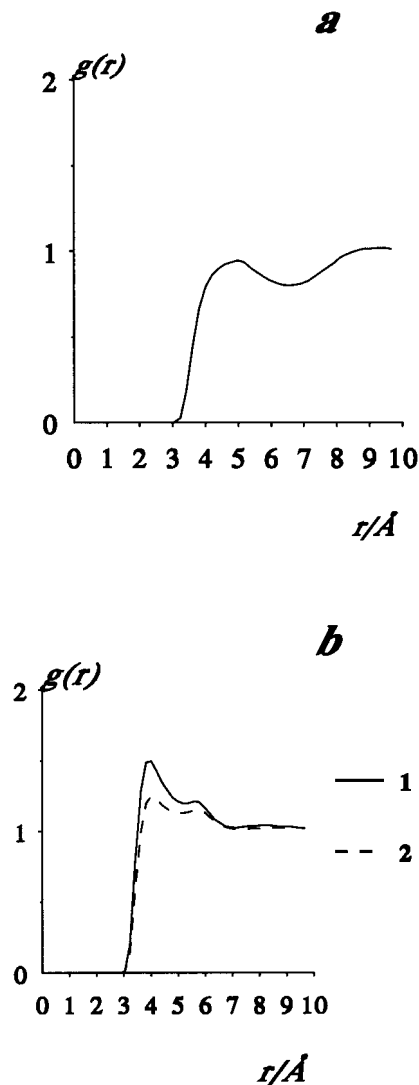


Figure 4. CH_3 (in ethane molecule)- CH_2 (in ethanol molecule) correlation function in the liquid phase at $p = 7.83$ MPa with $x_{\text{C}_2\text{H}_6} = 0.52$ (a) and $\text{CH}_3\text{-CH}_3$ correlation function for ethane molecules (b): (1) in the liquid phase at $p = 7.83$ MPa ($x_{\text{C}_2\text{H}_6} = 0.52$); (2) in the vapor phase at $p = 7.83$ MPa ($x_{\text{C}_2\text{H}_6} = 0.93$).

of those subsystems, all components added together. In fact, we observe quite strong dependence of the calculated compositions, energies, and densities of coexisting phases on the ratio of the number of particles in these phases at $p = 7.83$ MPa. For the simulation results given in this paper, the number of particles is about 1000 in the liquid phase and somewhat higher than 700 in the vapor phase. Meanwhile, the dependence of the results of the *total* number of particles in the model system ("standard" system-size effect) is much weaker, as we have seen after performing an additional simulation run for the smaller system (with 512 particles). Thus, we can suppose that choosing different total numbers of particles in the system as a whole at different pressures will not affect significantly the reliability of the computer simulation results, if we do not allow the number of molecules in one of the coexisting phases to become much greater than in other phase.

As for the agreement of the Monte Carlo results with the experimental data, one could assume that some changes in the values of the model potential parameters would allow to improve it for pressures closer to the critical point. Van Leeuwen⁸ made such an adjustment of the parameters for pure alcohols. As the model potentials for pure components of the binary systems

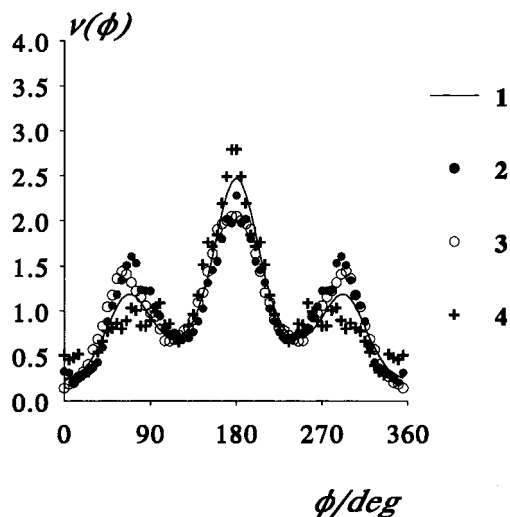


Figure 5. Conformational distribution of ethanol molecules: (1) in the ideal gas; (2) in the liquid phase at $p = 1.70$ MPa ($x_{\text{C}_2\text{H}_6} = 0.086$); (3) in the liquid phase at $p = 7.83$ MPa ($x_{\text{C}_2\text{H}_6} = 0.52$); (4) in the vapor phase at $p = 7.83$ MPa ($x_{\text{C}_2\text{H}_6} = 0.74$).

were already adjusted to fit the experimental data for these pure substances, it would be natural to try varying, first of all, the parameters for “mixed” interactions, for example, by modification of the Lorentz–Berthelot rules. However, the “number of degrees of freedom” in such variations would be high and their physical meaning would be somewhat unclear. The situation is complicated still more as some authors introduce the dependence of model potential parameters on the simulation conditions, such as temperature or density.²⁰ Perhaps, more extensive simulations of a number of alcohol- and hydrocarbon-containing systems at different temperatures would allow to obtain more reliable values of “transferable” group–group interaction parameters.

Hydrogen bonding characteristics (Table 3) for $\text{C}_2\text{H}_5\text{OH}$ molecules show that the increase of ethane content in the liquid phase has only a weak influence on both the average number of hydrogen bonds per ethanol molecule n_{av} and the percentage α_n of $\text{C}_2\text{H}_5\text{OH}$ molecules forming n H-bonds ($0 \leq n \leq 3$). This is different from the behavior of the methanol–ethane system³ where the lyophobic effect, caused by the presence of nonpolar hydrocarbon, results in notably lower branching of chains of associated methanol molecules (decrease of α_3 and increase of α_2), although n_{av} does not change significantly. A possible explanation of a less visible lyophobic effect in the case of ethanol refers to a longer hydrocarbon tail in the $\text{C}_2\text{H}_5\text{OH}$ molecule; so, ethane molecules can place themselves relatively freely in regions occupied by the tails, and the behavior of polar hydroxyl heads is less influenced by them. However, it should be noted that some lyophobic effect is quite visible, manifesting itself particularly in the decrease of the content of “branching points” in the chains of associated molecules (that is, the decrease of α_3).

More definite conclusions can be made from the atom–atom correlations in the liquid phase (Figures 3 and 4). Indeed, at relatively low concentrations of ethane, the functions describing $\text{CH}_2\text{--CH}_2$, O--O , H--H , and O--H correlations between ethanol molecules are almost identical to those obtained in ref 9 for pure $\text{C}_2\text{H}_5\text{OH}$ at 348 K. At higher C_2H_6 concentration, the first peaks of these functions increase significantly, while the values of these functions near their first minima do not become lower; in general, these correlation functions shift upward all over the first two coordination spheres. The $\text{CH}_3\text{--CH}_3$ correlation function for ethane molecules also has unusually high values

(this becomes still more obvious when the normal $\text{CH}_3\text{--CH}_3$ correlation function in the vapor, containing only small concentrations of ethanol, is also given, as in Figure 4b), while the CH_2 (in the $\text{C}_2\text{H}_5\text{OH}$ molecule)– CH_3 (in C_2H_6 molecule) correlation function does not even reach 1.0 in this range of distances. Such a behavior of the correlation functions can be explained by the tendency to microheterogeneity in the liquid solution of ethane in ethanol, that is, to the formation of nonpolar (ethane-rich) and polar (ethanol-rich, associated due to hydrogen bonding) cluster-like structures. In such a system, adding C_2H_6 can have only a slight effect on the spatial distribution of $\text{C}_2\text{H}_5\text{OH}$ molecules in ethanol associates, merely increasing the share of the space occupied by hydrocarbon fragments. This tendency to microheterogeneity is quite natural for the mixture of a hydrocarbon and an amphiphilic substance (for longer chain molecules such effects can lead to the formation of “reverse micelles”).

The conformational distribution of ethanol molecules in the liquid phase only slightly depends on the concentration of C_2H_6 (Figure 5). Jorgensen,⁷ having simulated liquid $\text{C}_2\text{H}_5\text{OH}$ at 298.15 K, found that, compared to the ideal gas (where $\nu(\phi)$ is proportional to $\exp(-U^{\text{tors}}(\phi)/kT)$), an increase of the fraction of gauche conformations and a decrease of the fractions of both trans and cis conformations take place in liquid, with a shift of gauche maxima of $\nu(\phi)$ toward trans. We also find the gauche population increased and the trans population decreased in the liquid phase; however, we do not observe the trans shift of the gauche maxima, and a visible decrease of the cis population is observed only in the concentrated solution of ethane at high pressure. Certainly, comparing $\nu(\phi)$ for pure liquid $\text{C}_2\text{H}_5\text{OH}$ at 298.15 K⁷ and for liquid solution of C_2H_6 in ethanol at 348.15 K (this work), one should take into account the temperature difference. In principle, the difference between the conformational distributions in the liquid phase and in the ideal gas, as it was noted in ref 7, can be explained by hydrogen bonding preferences: the oxygen atom in the gauche ethanol molecule forms the H-bond easier because in this case its “lone-pair” region (with which the hydrogen atom of another molecule would be associated) is less encumbered by the alkyl group than in the trans molecule. Jorgensen gave similar explanations also to less clear effects of cis population change and gauche maxima shift. It should be noted, however, that the model potential used both in ref 7 and in the present work does not include any explicit contribution of interaction between a methyl group of one $\text{C}_2\text{H}_5\text{OH}$ molecule and a hydrogen atom of the hydroxyl group of another molecule; so, the conformational behavior of alcohol molecules can reflect the peculiarities of the potential model only indirectly. As it was noted in ref 7, the details of the conformational distribution can be highly sensitive to small changes in the model (particularly in the values of Coulomb charges).

As for the conformational distribution in the vapor phase at $p = 7.83$ MPa (containing about 7% $\text{C}_2\text{H}_5\text{OH}$, that is, about 50 molecules), it shows higher percentage of trans conformations, rather “indistinct” distribution between cis and gauche conformations, and obvious trans shift of gauche maxima, in comparison with the ideal gas (Figure 5). These specific features can be explained by the tendency of alcohol molecules in vapor to form, because of hydrogen bonding, relatively small clusters, where $\nu(\phi)$ can differ significantly from $\nu(\phi)$ in the bulk liquid.

Conclusions

The results of this work as a whole allow to conclude that the Gibbs ensemble MC simulation using relatively simple model potentials allows to calculate the phase behavior of an

ethanol–ethane system at a temperature higher than the critical point of ethane but lower than that of ethanol, the agreement with experiment being satisfactory at pressures far enough from the critical value. Rather subtle details of structure of the liquid and dense vapor can be studied in such a simulation. At the same time, at higher pressures (closer to the critical point) serious difficulties arise, caused both by bad ergodicity of the system (forcing to generate exceptionally long Markov chains of configurations) and by very high sensitivity of the quantitative characteristics of the system behavior in the near-critical region to the details of model potential. Similar problems are even more important for more complex systems containing higher alcohols and hydrocarbons. Most probably, their simulation will require “configurational bias” or other modifications of the general MC algorithm.

Acknowledgment. We thank Prof. S. W. de Leeuw for useful collaboration and the possibility to use the computer facilities of the Technical University of Delft (The Netherlands) for these calculations. We are thankful to the Russian Foundation of Basic Research for financial support (Grant 96-15-97399).

References and Notes

- (1) Gotlib, I. Yu.; Piotrovskaya, E. M. *Russ. J. Phys. Chem.* **1992**, *66*, 74.
- (2) Piotrovskaya, E. M.; Gotlib, I. Yu. *Russ. J. Phys. Chem.* **1994**, *68*, 1756.
- (3) Gotlib, I. Yu.; Piotrovskaya, E. M. *Fluid Phase Equilib.* **1997**, *129*, 1.
- (4) Brunner, E. *J. Chem. Thermodyn.* **1985**, *17*, 871.
- (5) Brunner, E.; Hültschmidt, W. *J. Chem. Thermodyn.* **1990**, *22*, 73.
- (6) Lustig, R.; Toro-Labbé, A.; Steele, W. A. *Fluid Phase Equilib.* **1989**, *48*, 1.
- (7) Jorgensen, W. L. *J. Phys. Chem.* **1986**, *90*, 1276.
- (8) Van Leeuwen, M. E. *Mol. Phys.* **1996**, *87*, 87.
- (9) Gao, J.; Habibollahzadeh, D.; Lei, Sh. *J. Phys. Chem.* **1995**, *99*, 16460.
- (10) Saiz, L.; Padró, J. A.; Guàrdia, E. *J. Phys. Chem. B* **1997**, *101*, 78.
- (11) Kriebel, C.; Müller, A.; Winkelmann, J.; Fisher, J. *Mol. Phys.* **1995**, *84*, 381.
- (12) Vrabec, J.; Fisher, J. *Int. J. Thermophys.* **1996**, *17*, 889.
- (13) Mezei, M. *Mol. Simul.* **1992**, *9*, 257.
- (14) Fischer, J.; Lustig, R.; Breitenfelder-Manske, H.; Lemming, W. *Mol. Phys.* **1984**, *52*, 485.
- (15) Smirnova, N. A.; Victorov, A. I. *Fluid Phase Equilib.* **1987**, *34*, 235.
- (16) Victorov, A. I.; Fredenslund, A. *Fluid Phase Equilib.* **1991**, *66*, 77.
- (17) Deák, A.; Victorov, A. I.; De Loos, Th. W. *Fluid Phase Equilib.* **1995**, *107*, 277.
- (18) Panagiotopoulos, A. Z. *Int. J. Thermophys.* **1994**, *15*, 1057.
- (19) Valleau, J. P. *J. Chem. Phys.* **1998**, *108*, 2962.
- (20) De Pablo, J. J.; Bonnin, M.; Prausnitz, J. M. *Fluid Phase Equilib.* **1992**, *73*, 187.